PUBLICATION IV

Optimized Design and Process for Making a DC Voltage Reference Based on MEMS

In: IEEE Transactions on Instrumentation and Measurement 2005. Vol. 54, pp. 563–566.

Optimized Design and Process for Making a DC Voltage Reference Based on MEMS

Anu Kärkkäinen, Shakil A. Awan, Jukka Kyynäräinen, Panu Pekko, Aarne S. Oja, and Heikki Seppä

***Abstract*—A micromechanical moving plate capacitor has been designed and fabricated for use as a dc voltage reference. The reference is based on the characteristic pull-in property of a capacitive microelectromechanical system (MEMS) component. The design is optimized for stability. A new silicon-on-insulator (SOI) process has been developed to manufacture the component. We also report on improved feedback electronics and the latest measurement results.**

***Index Terms*—Capacitive sensors, feedback electronics, microelectromechanical systems (MEMS), micromachining, silicon-on-insulator (SOI).**

I. Introduction

THE characteristic pull-in voltage of a microelectromechanical system (MEMS) moving plate capacitor depends only, in principle, on its spring constant and geometrical properties. The pull-in voltage of a capacitive MEMS component has been proposed for use as a dc voltage transfer standard in metrology [1]–[6]. The moving plate of a MEMS parallel plate capacitor, suspended by single crystal silicon springs, can be very stable in comparison with, for example, Zener diodes. The latter have an inherent $1/f$ noise and long term stability limitations [7]. The MEMS capacitive devices can be designed to operate at any voltage up to several hundred volts. In theory, the device stability is limited by mechanical noise [5].

The major challenge in the MEMS dc voltage reference development is to achieve high stability, preferably better than $1\ \mu\mathrm{V/V}$/year. The major improvements introduced in the new design, compared to the earlier published results, are the use of stress-free silicon-on-insulator (SOI) manufacturing process, metallization of both electrode surfaces, and built-in voltage compensation. The major factors effecting the pull-in voltage stability are the spring constant k and the gap d. The spring is made out of single crystal silicon resulting in a very stable spring constant k with time. However, Young's modulus has a temperature coefficient of $-60\ \mu\mathrm{V/V/K}$, which effects the temperature dependence of the spring constant. But even a 10 to 20 times higher temperature coefficient can arise from the component mounting. The sensor needs to be stabilized for temperature or temperature compensated.

Longitudinal and vertical residual stress inherent in an epi poly process, strongly influences the gap and, hence, the time and temperature stability of the device [8]. A new SOI process has been developed for fabrication of a series of components. The seesaw design, a rectangular plate suspended by torsion springs at the symmetry axis, is selected for the component, because it is less sensitive to stress or vibration than a cantilever or beam type capacitor. Stress-free mounting of the component is also essential.

Also, various electrode surface phenomena can have an effect on the pull-in voltage. The charging effect can be reduced by metallizing the electrode surfaces, which is enabled by the new process as well, albeit with significantly increased complexity.

In addition, the built-in voltage of the component is temperature dependent and, hence, a source of instability. The built-in voltage temperature dependence can be eliminated in the first order by applying a compensating dc voltage on the moving plate or using "split" electrodes, explained later in detail.

In our previous work [4], the underlying dc voltage reference stability was found to be $1\ \mu\mathrm{V/V}$ only after subtracting the measured drift of the pull-in voltage from the curve fitted to the data. The actual drift was $-6000\ \mu\mathrm{V/V}$ over 60 h.

II. Principle of Operation

When a dc voltage V is applied across a moving plate capacitor, the capacitor plates are pulled towards each other by an electrostatic force $F_\mathrm{e} = C_0 V^2 d/2(d-x)^2$, where x is the deflection, d is the gap at $x = 0$, $C_0 = \varepsilon A/d$ is the capacitance at $x = 0$, ε is the dielectric constant, and A the capacitor plate area. The mechanical force $F_\mathrm{m} = -kx$, where k is the spring constant, acts as a restoring force on the plate position. The maximum dc voltage across the capacitor is known as the pull-in voltage

$$V_\mathrm{pi} = \sqrt{\frac{8kd^2}{27C_0}} \tag{1}$$

which occurs when $x = d/3$, as can be seen in Fig. 1. The displacement can be stabilized at that point by a force feedback loop. The pull-in voltage can be used as a dc voltage reference. Small deviations in the plate deflection Δx, near $x = d/3$, have only a second order effect in the reference voltage $\Delta V/V_\mathrm{pi} \sim 27/4\ (\Delta x/d)^2$ which makes the pull-in point excellent for the reference use.

Manuscript received July 2, 2004; revised October 29, 2004. This work was supported in part by the EMMA project (IST-2000-28261) funded by the European Commission Framework V Program and by the National Technology Agency of Finland. S.A. Awan would like to acknowledge support from the Glazebrook Fellowship Award and the NPL Strategic Research 9SRPE140 Project to attend VTT as Guest Researcher between January and March 2004.

A. Kärkkäinen, J. Kyynäräinen, P. Pekko, A. S. Oja, and H. Seppä are with the VTT Information Technology, Microsensing, FIN-02044 VTT, Finland (e-mail: anu.karkkainen@ vtt.fi).

S. A. Awan is with the Division of Enabling Metrology, National Physical Laboratory, Queens Road, Teddington, Middlesex, TW11 0LW, U.K. (e-mail: shakil.awan@npl.co.uk).

Digital Object Identifier 10.1109/TIM.2004.843097

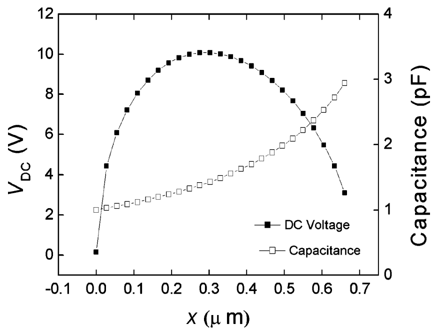

Fig. 1. Calculated eigencurve for a component with 10-V pull-in voltage ($k = 405$ N/m, $d = 1$ μm, $C_0 = 1.2$ pF).

III. Component Manufacturing

A new fabrication process has been developed in order to realize the metallization of both capacitor surfaces. The approach chosen is based on aligned direct bonding of separately metallized and patterned wafers. The device wafer was a SOI wafer with a 20-μm-thick device layer and a 1-μm buried oxide layer and the substrate wafer was a 380 μm-thick double-side polished Si wafer. Both of the wafers were boron-doped and the resistivity was 0.015 to 0.02 Ωcm. The metal electrodes are placed in wells to avoid problems in wafer bonding. The well depth and oxide thickness of the substrate wafer define the gap height, which is 1 μm.

The process consists of four parts: 1) processing the electrodes to the device wafer; 2) processing the electrodes to the substrate wafer; 3) low-temperature fusion bonding of the wafers; and 4) inductively coupled plasma (ICP) etching the bonded pair when the moving part is released. The process diagram is shown in Fig. 2. The process requires 10 lithography steps.

The most critical step in the process is the wafer bonding. If the bonding surface quality (surface roughness and freedom from contaminants) is inadequate, large nonbonded areas can be observed in optical or acoustical measurements. In the worst case, the wafers will not bond at all. To keep the surfaces in bondable condition, careful process planning and frequent cleaning procedures are demanded throughout the fabrication. Also, trapped gas bubbles between the bonded wafers can cause large nonbonded areas, as experienced in our process. The component yield from the successfully bonded areas was very good.

IV. Component Design

The basic design of the dc voltage reference is illustrated in Fig. 3. The top actuator electrode (550×800 μm) is suspended at its center of mass with two 180-μm-long silicon springs. The bottom of the moving plate actuator is coated with sputtered molybdenum, and the top of the lower fixed plate is coated with sputtered aluminum. The upper plate moves in torsion mode and the mechanical resonance frequency is typically 30 kHz. The component was designed to be as large as the manufacturing process allowed in order to achieve high capacitance values.

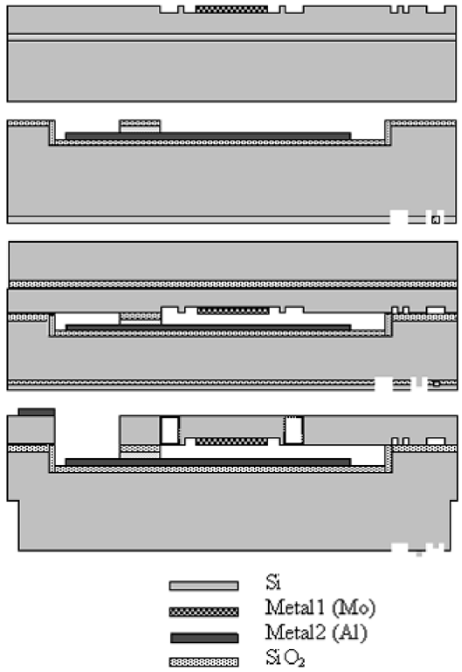

Fig. 2. Major process steps for fabricating the MEMS dc voltage reference.

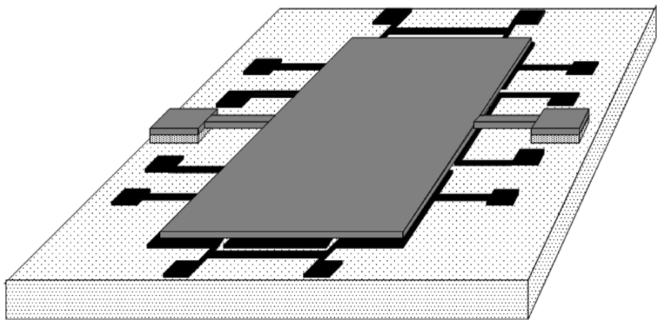

Fig. 3. Silicon-on-insulator (SOI) parallel plate capacitive seesaw component.

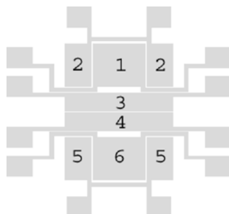

Fig. 4. Bottom electrodes of the component. Double contact pads are needed for the four terminal pair measurements.

The bottom electrode is divided into four sections as shown in Fig. 4. The two sections in the middle are the sense electrodes for displacement control (3 and 4). The top electrodes (1 and 2) are used for actuating the seesaw to the pull-in position while the other electrodes (5 and 6) are grounded. The built-in voltage (V_{bi}), which originates from the work function difference of the metal electrode and the silicon spring, can be compensated by splitting the actuation electrode into two equal sections and applying slightly different voltages with opposite polarity on the electrodes. If a positive voltage V_{p} is applied to electrode 1, and a negative voltage V_{n} is applied to electrode 2 so that $V_{\mathrm{p}} = V_0 + V_{\mathrm{bi}}$ and $V_{\mathrm{n}} = -V_0 + V_{\mathrm{bi}}$, with V_0 being

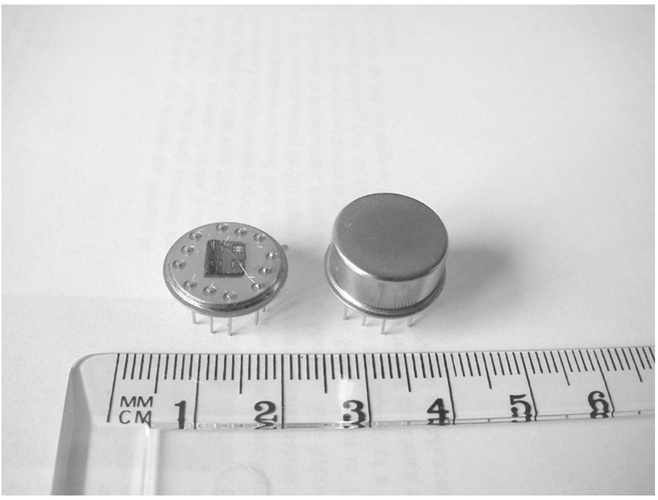

Fig. 5. Component mounted on a TO-8 can and a hermetically encapsulated component.

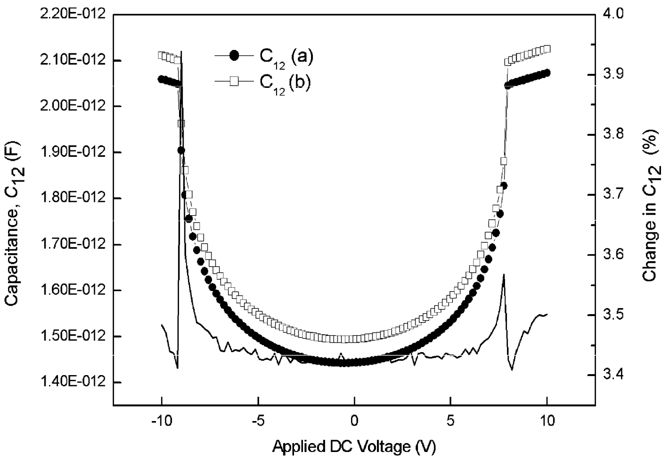

Fig. 6. Characteristic C–V curves (including repeatability a and b) of a component showing the measured pull-in voltage and the built-in voltage (the shift of the minima from 0 V). The solid curve is the change in C_{12} repeatability.

the average of positive and negative pull-in voltage values, the electrostatic force F_{e}, $F_{\mathrm{e}} \propto V_{\mathrm{p}}^2 + V_{\mathrm{n}}^2 \approx 2V_0^2$ is independent of V_{bi} in the first order.

Metal surfaces can be very hydrophilic. If there are any residual chemicals from the manufacturing process inside the sensor enclosure, they can out gas with time and effect the device stability. Thus, the component was encapsulated into a hermetically sealed TO-8 can containing 1 atm nitrogen gas. Atmospheric pressure mechanically damps the seesaw electrode, which is also necessary for the stability of the feedback electronics. Fig. 5 shows a component glued in a TO-8 can and a hermetically encapsulated component.

V. Capacitance–Voltage Curve

The characteristic C–V curves of a component are shown in Fig. 6 including repeatability measurements. From Figs. 3 and 4, it is possible to define two capacitances, C_{12} and C_{56}, which exist between the top electrode and the two fixed lower electrodes. The C–V curves of a component were determined by measuring the change in capacitance C_{12} while the dc voltage was increased until the pull-in voltage was reached. Capacitance was measured using a HP 4284A four terminal-pair impedance bridge at 1 MHz and 0.5 $\mathrm{V_{rms}}$, with the two sections of the lower electrode shorted together. The component capacitance, at $V_{\mathrm{dc}} = 0$, was from 1.4 to 1.9 pF, which the HP bridge could resolve to approximately 10 aF. From the C–V curves, both the pull-in voltage and the dc bias voltage needed for the split electrodes, to compensate the built-in voltage, were determined. The repeatability measurements demonstrate that the pull-in and the built-in voltages of these types of components do not change with cycling of the applied dc voltage, and only the shunt capacitance changes due to ambient temperature variations.

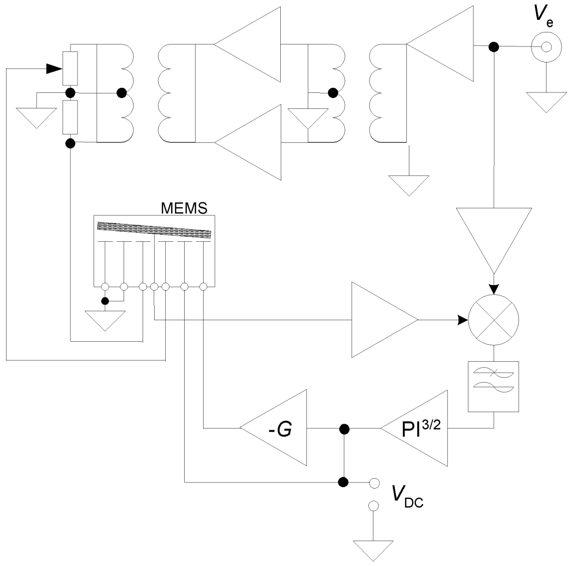

Fig. 7. Feedback electronics used to monitor the stability of the dc voltage reference.

VI. Experimental Setup and Feedback Electronics

The schematic of the experimental setup and the force feedback electronics used to monitor the stability of the device is shown in Fig. 7. The elastically supported seesaw electrode is symmetrically positioned above six rigid electrodes to form six capacitances. The position of the seesaw electrode is monitored by the ac capacitive bridge formed of the innermost electrodes (3, 4). The ratio of the ac voltage levels of the two arms is adjusted so that the total current at the seesaw vanishes at $x = d/3$. The deflection of the seesaw is stabilized at $x = d/3$ by controlling the dc voltage on the two rightmost electrodes (1, 2). These electrodes have equal areas and are located equidistant from the springs. Since the electrostatic force is independent of the voltage polarity, the built-in voltage can be compensated by applying slightly different voltages with opposite polarities to the electrodes as discussed in Section IV. The voltage difference is controlled with gain G. The feedback voltage is the result of an output voltage from the bridge, which is proportional to the seesaw fluctuations away from the set value of $x = d/3$. This voltage is combined with a reference voltage from the bridge oscillator in a mixer. The resultant output of the mixer is a dc voltage with superimposed harmonic components of the input voltages. The harmonics of the fundamental are filtered using a

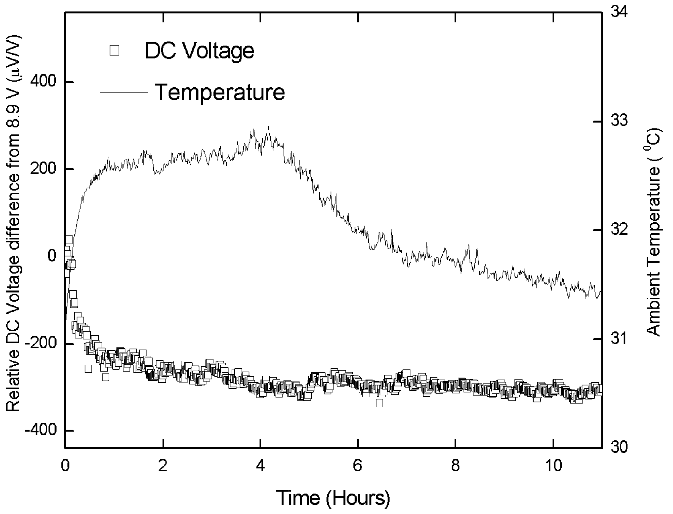

Fig. 8. Stability of the dc voltage reference (component S7/SAW6) over 11 h, showing best stability of 60 $\mu\mathrm{V/V}$. The solid curve shows the corresponding ambient temperature recorded during the measurements.

lowpass filter, leaving only a dc signal. This is fed to a $\mathrm{PI}^{3/2}$ controller in the feedback loop which restores the position of the seesaw electrode to the set value of $x = d/3$. This controller output voltage can be used as the dc reference voltage.

VII. DC Voltage Experiment

Fig. 8 shows a dc voltage reference measurement result. After the initial rapid change in the reference voltage, the device stabilizes at approximately 60 $\mu\mathrm{V/V}$ stability over the next 10 h. Fig. 8 does not include any ambient temperature corrections to the measured dc voltage reference. Therefore, the inherent stability of the device is likely to be better. Further improvements are still needed for component packaging and feedback electronics.

VIII. Conclusion

We have designed a new MEMS component optimized for a dc voltage reference use and developed a manufacturing process for it. The main target was to eliminate surface charging and mechanical stress effecting the component stability. The first experimental results of the new device show an order of magnitude improvement with respect to earlier work. Further work will include improvements in the feedback electronics as well as stress-free mounting of the component.

References

[1] M. Suhonen, H. Seppä, A. S. Oja, M. Heinilä, and I. Näkki, "AC and DC voltage standards based on silicon micromechanics," in *Proc. CPEM Conf. Dig.*, 1998, pp. 23–24.

[2] H. Seppä, A. S. Oja, and M. Suhonen, "Micromechanical AC and DC Voltage Reference System," W.O. Patent, PCT/FI99/00553, WO 00/02110, 1999.

[3] A. S. Oja, J. Kyynäräinen, and H. Seppä, "A micromechanical DC voltage reference," in *Proc. CPEM Conf. Dig.*, 2000, pp. 701–702.

[4] J. Kyynäräinen, A. S. Oja, and H. Seppä, "Stability of microelectromechanical devices for electrical metrology," *IEEE Trans. Instrum. Meas.*, vol. 50, no. 6, pp. 1499–1503, Dec. 2001.

[5] H. Seppä, J. Kyynäräinen, and A. S. Oja, "Microelectromechanical systems in electrical metrology," *IEEE Trans. Instrum. Meas.*, vol. 50, no. 2, pp. 440–444, Apr. 2001.

[6] L. A. Rocha, E. Cretu, and R. F. Wolffenbuttel, "Stability of a micromechanical pull-in voltage reference," *IEEE Trans. Instrum. Meas.*, vol. 52, no. 2, pp. 457–460, Apr. 2003.

[7] P. Helistö and H. Seppä, "Measurement uncertainty in the presence of low-frequency noise," *IEEE Trans. Instrum. Meas.*, vol. 50, no. 2, pp. 453–456, Apr. 2001.

[8] L. A. Rocha, E. Cretu, and R. F. Wolffenbuttel, "Analysis and analytical modeling of static pull-in with application to MEMS-based voltage reference and process monitoring," *J. Microelectromech. Syst.*, vol. 13, pp. 342–354, 2004.